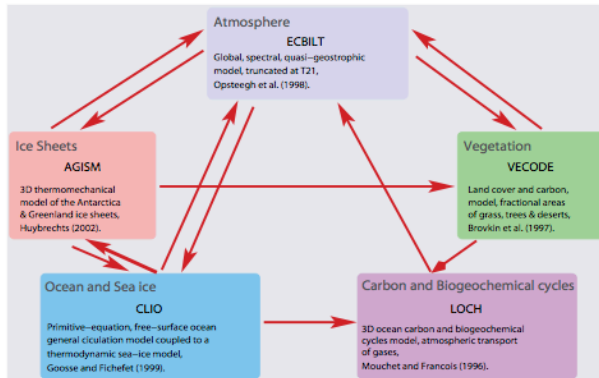**Fig. 1.** Sketch of the LOVECLIM model showing the interactions between the five components.

LOVECLIM (Fig. 1) is a three-dimensional Earth system model of i1n6t1e6rmediate complexity (EMIC, Claussen et al., 2002), i.e. its spatial resolution is coarser than that of state-of-the-art climate General Circulation Models (GCMs) and its representation of physical processes is simpler. In LOVECLIM, the most important simplifications are applied in the atmospheric component because it is usually the most demanding one in terms of computing time in GCMs. Thanks to those modelling choices, LOVECLIM is much faster than GCMs
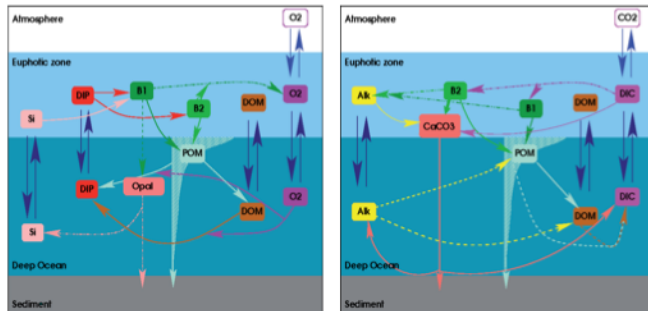

Fig. 5. Schematic representation of the main processes described in the LOCH model (Mouchet, 2010). The left panel focuses on purely biological processes, while the right panel shows the processes affecting the ocean carbon cycle. Up and down blue arrows represent transport processes (advection, diffusion, etc). Transported variables include dissolved inorganic carbon (DIC), alkalinity (Alk), dissolved inorganic phosphorus (DIP), dissolved organic matter (DOM), oxygen (O_2) and silica (Si). At the air-sea interface CO_2 and O_2 are exchanged with the atmosphere. B1 stands for opal building phytoplankton biomass and B2 represents the biomass of phytoplankton not relying on silica for growth (please note the inversion of B1 and B2 boxes between panels). POM decays at depth either as DOM or DIP. The flux of POM is governed following a power law function of the depth. Opal dissolves while sinking to the bottom. Calcareous shells ($CaCO_3$) reach the deepest layer where chemical conditions drive their dissolution or preservation. Fluxes to sediments, where permanent preservation prevails in this version, are also represented. Rivers (not illustrated) carry Si, DOM, DIC and Alk to the ocean.

CLIMATE CHANGE
Nonlinear climate sensitivity and its implications for future greenhouse warming

Tobias Friedrich,1* Axel Timmermann,1 Michelle Tigchelaar,2 Oliver Elison Timm,3 Andrey Ganopolski4 (PIK)

Abstract
Global mean surface temperatures are rising in response to anthropogenic greenhouse gas emissions.

The magnitude of this warming at equilibrium for a given radiative forcing—
  - referred to as specific equilibrium climate sensitivity (S)—
is still subject to uncertainties.

We estimate global mean temperature variations and S using a 784,000-year-long field reconstruction of sea surface temperatures (SST) and a transient paleoclimate model simulation.

Our results reveal that S is strongly dependent on the climate background state,
  - with significantly larger values attained during warm phases.

Using the Representative Concentration Pathway 8.5 for future greenhouse radiative forcing, we find
  - that the range of paleo-based estimates of Earth's future warming by 2100 CE overlaps with the upper range of climate simulations conducted as part of the Coupled Model Intercomparison Project Phase 5 (CMIP5).
  - that within the 21st century, global mean temperatures will very likely exceed maximum levels reconstructed for the last 784,000 years.
On the basis of temperature data from eight glacial cycles, our results provide an independent validation of the magnitude of current CMIP5 warming projections.

DISCUSSION
Constraining the magnitude of future greenhouse warming is critical for risk assessment and adaptation strategies. Using our combined proxy/modeling approach based on the 784-ka SST data and applying it to the projected atmospheric CO2 concentrations and radiative forcings results in SAT changes that overlap with the upper range of current CMIP5 RCP8.5 projections.
  - The resulting paleodata-based estimate of surface warming by 2100 CE is ~16% higher than the CMIP5 ensemble mean projection.
  - Our results suggest that a global surface temperature increase of 4 K by 2100 CE (compared to the PI reference value) is likely. Furthermore,
  - our analysis demonstrates that in the case of unabated anthropogenic CO2 emissions, the maximum long-term global mean SATs ever obtained during the past 8 glacial cycles will very likely be surpassed within the 21st century.
  - According to our results, the Earth's specific equilibrium climate sensitivity is a function of the background climate with a substantially higher sensitivity during warm phases.
  - It remains unclear whether this relationship will hold in climates substantially warmer than during the last 8 glacial cycles. Therefore, we restrict our warming estimate to the 21st century and refrain from applying our method to potential greenhouse warming in a more distant future.
  - Uncertainties associated with past temperature and radiative forcing data are still relatively large.
    - These uncertainties directly affect the estimate of S, limiting a more accurate paleo-based projection of future greenhouse warming.
    - However, our independent future warming estimates and their associated uncertainty ranges overlap with the CMIP5 RCP8.5 projections, thus providing further evidence for the climate model–based warming projections.

Influence of Anthropogenic Climate Change on Planetary Wave Resonance and Extreme Weather Events

Michael E. Mann[1], Stefan Rahmstorf[2], Kai Kornhuber[2], Byron A. Steinman[3], Sonya K. Miller[1] & Dim Coumou[2,4]
1Department of Meteorology and Atmospheric Science, Pennsylvania State University, University Park, PA USA. 2Earth System Analysis, Potsdam Institute for Climate Impact Research, Potsdam,

Germany. 3Department of Earth and Environmental Sciences and Large Lakes Observatory, University of Minnesota Duluth, Duluth, Minnesota, USA. 4Institute for Environmental Studies (IVM), VU University Amsterdam, Amsterdam, The Netherlands. Correspondence and requests for materials should be addressed to M.E.M. (email: mann@psu.edu)

Abstract
Persistent episodes of extreme weather in the Northern Hemisphere summer have been shown to be associated with the presence of high-amplitude quasi-stationary atmospheric Rossby waves within a particular wavelength range (zonal wavenumber 6–8). The underlying mechanistic relationship involves the phenomenon of quasi-resonant amplification (QRA) of synoptic-scale waves with that wavenumber range becoming trapped within an effective mid-latitude atmospheric waveguide. Recent work suggests an increase in recent decades in the occurrence of QRA-favorable conditions and associated extreme weather, possibly linked to amplified Arctic warming and thus a climate change influence.
-    Here, we isolate a specific fingerprint in the zonal mean surface temperature profile that is associated with QRA-favorable conditions.
-    State-of-the-art ("CMIP5") historical climate model simulations subject to anthropogenic forcing display an increase in the projection of this fingerprint that is mirrored in multiple observational surface temperature datasets.
-    **Both the models and observations suggest this signal has only recently emerged from the background noise of natural variability.**

In summary,
our analysis of both historical model simulations and observational surface temperature data, strongly suggests that anthropogenic warming is impacting the zonal mean temperature profile in a manner conducive to wave resonance and a consequent increase in persistent weather extremes in the boreal summer. Combined with other additional proposed mechanisms for climate change impacts on extreme weather, this adds to the weight of evidence for a human influence on the occurrence of devastating events such as the 2003 European heat wave, the 2010 Pakistan flood and Russian heat wave, the 2011 Texas heat wave and recent floods in Europe.
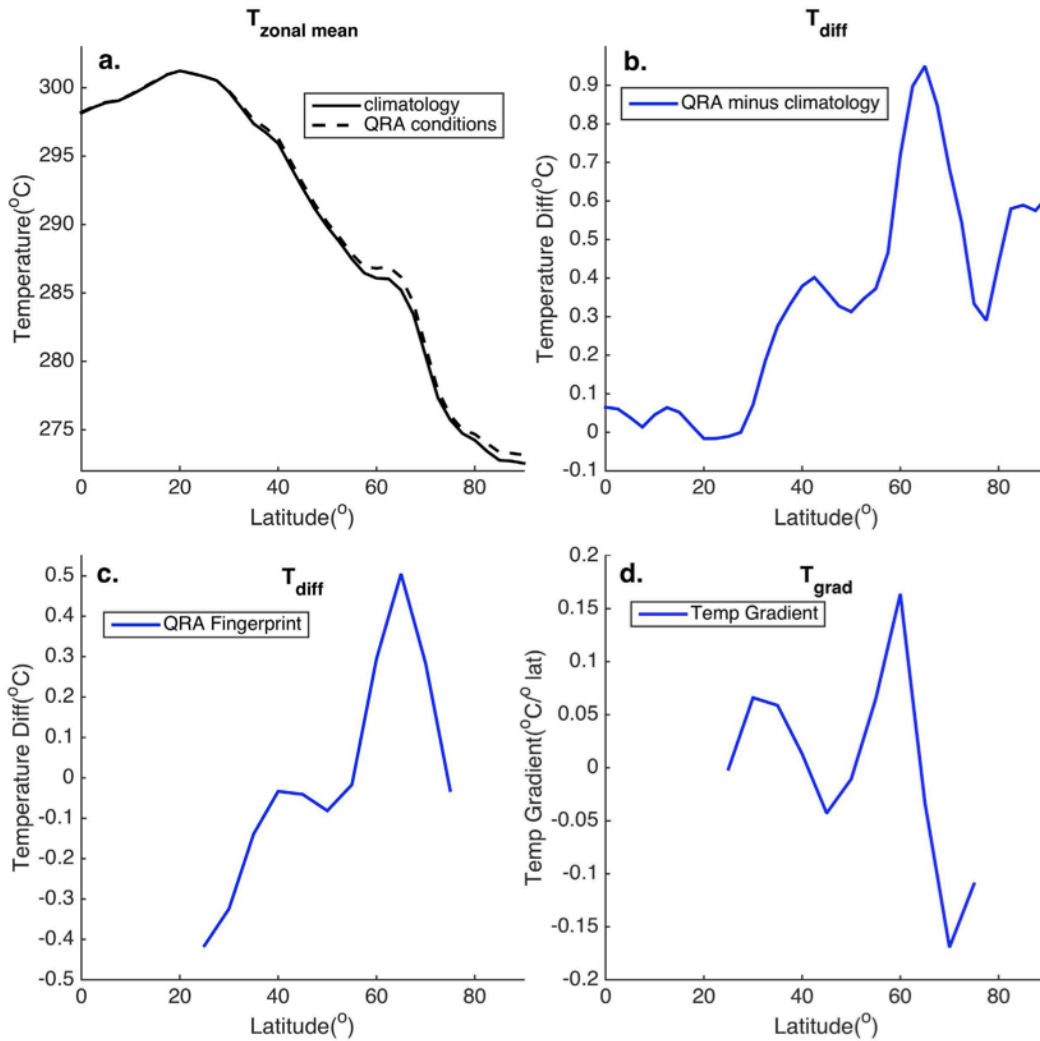
Details
We used the Coupled Model Intercomparison Project Phase 5 (CMIP5) historical experiment38 multimodel ensemble simulations, including both the
-    anthropogenic+natural forced simulations (N = 164 realizations; M = 48 models) and
-    anthropogenic-only forced simulations (N = 40 realizations; M = 10 models)
spanning 1861–2005 (Table S1). Each physics version of a model was considered a separate model.

The analysis was limited to the common time period of overlap for all models and realizations (1861– 2005). Those with a start year later than 1861 were not included in the analysis. We used a simple area-weighted average to create zonal means at a 5° interval.

Zonal Temps (all-forcing)

a.

Temperature(°C)
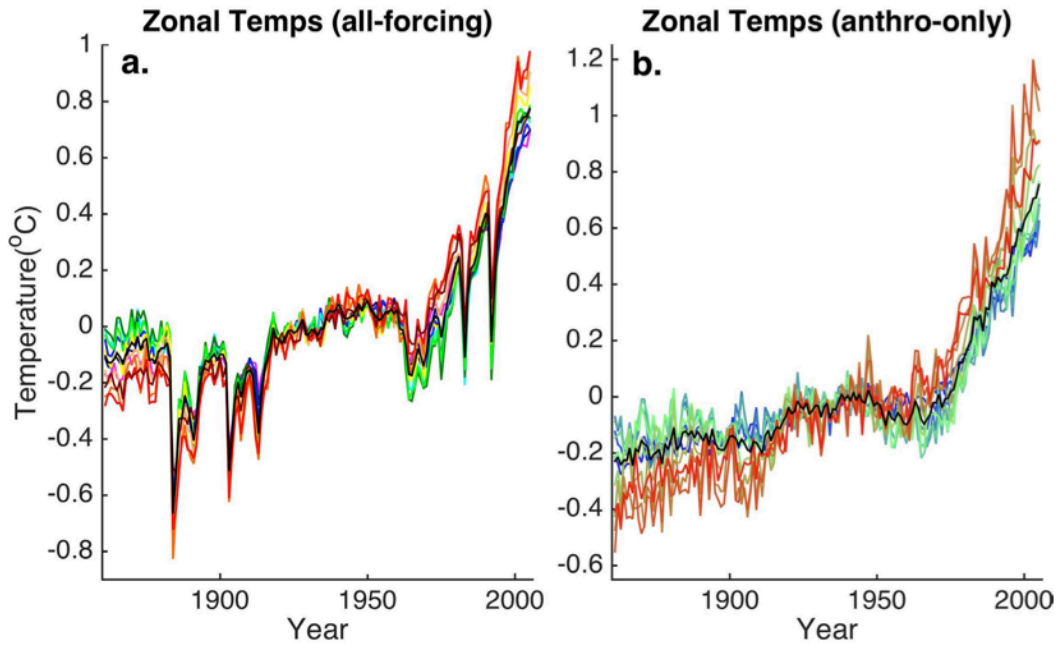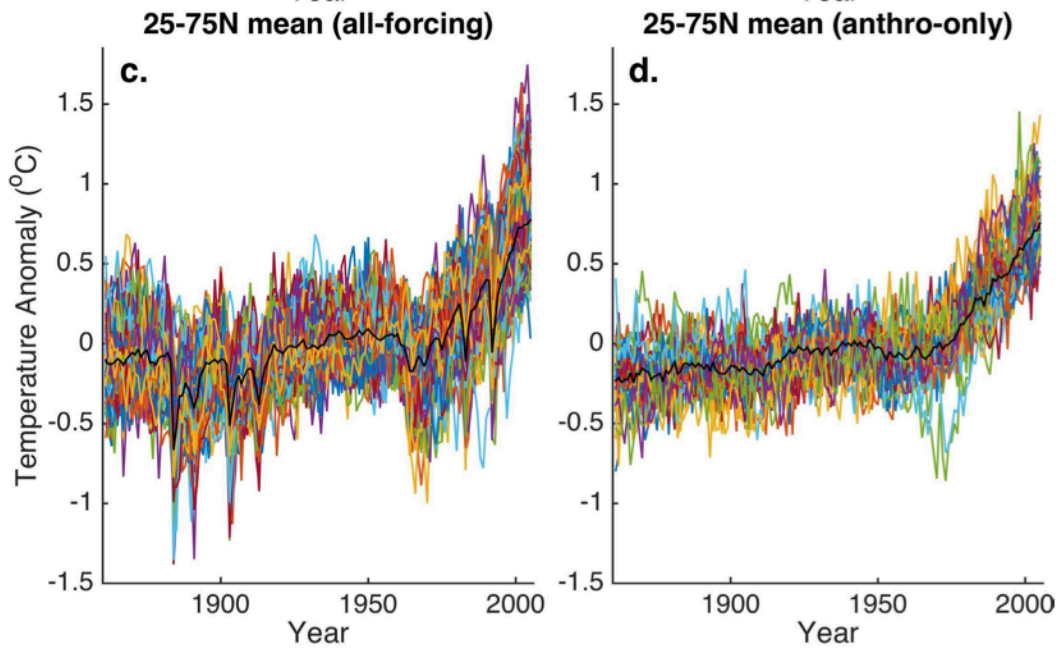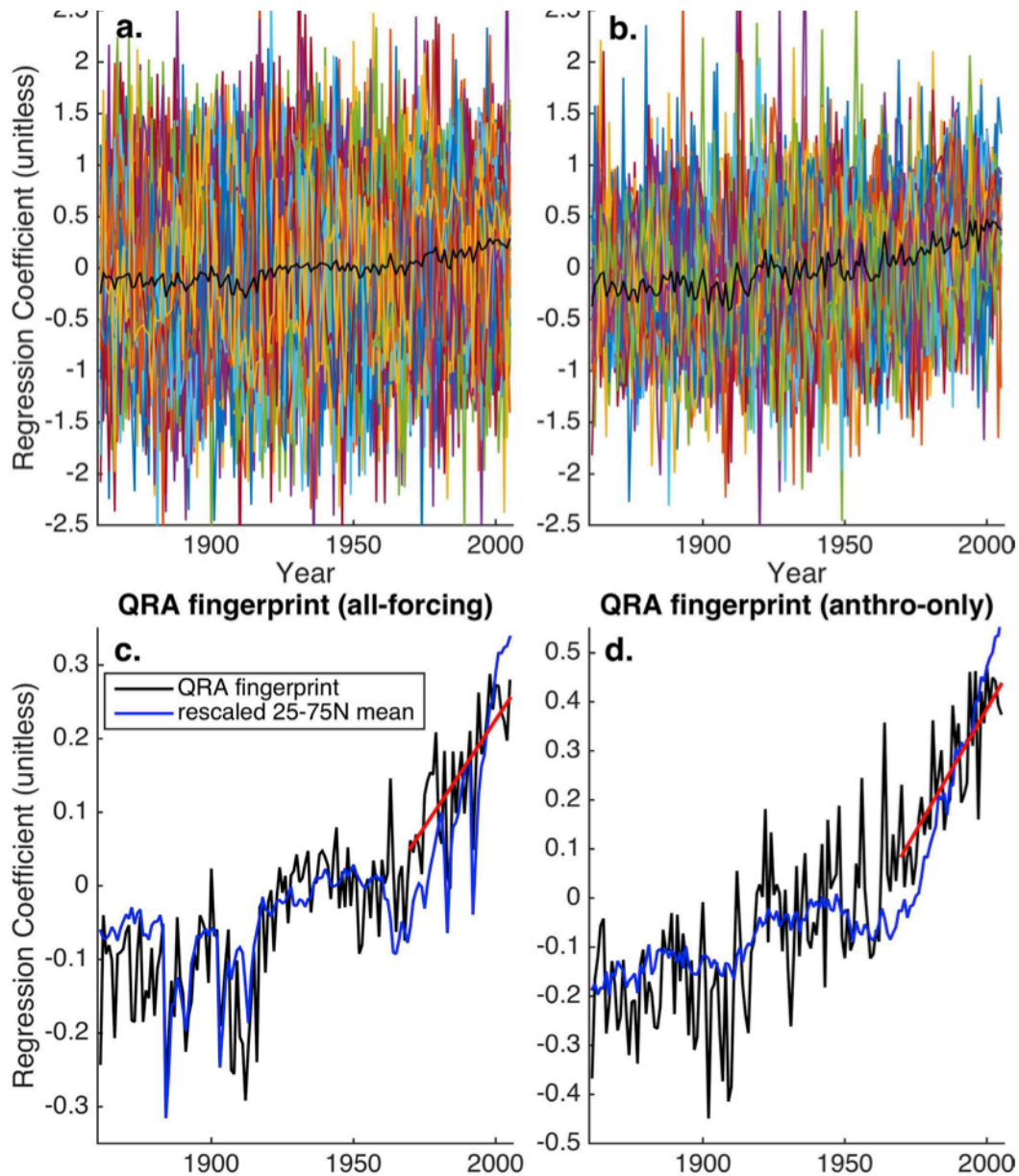
Year

Zonal Temps (anthro-only)

b.

Year

Figure 2 a & b
variability from zone to zone (zone separation: 5 degrees latitude)
what is the warming in a zone?
latitude (zone) = color - zones's mean: black
curve = multimodel mean temperature for a chosen zone

25-75N mean (all-forcing)

c.

Temperature Anomaly (°C)

Year

25-75N mean (anthro-only)

d.

Year

Figures 2c & d.
Model dependent single CMIP5 model temperatures averaged over latitude range 25–75N (CMIP5 historical simulations)
So this is the AR5 Fig. 2.3 band resolved into single CMIP5 models
internal natural climate variability from model to model: how do warming predictions vary from model to model?
model = color - multimodel mean: black
curve = temperature averaged over 25-75N zone, given by a chosen model

CMIP5 multimodel simulations:
164 in Fig. 2c (40 in Fig. 2d) realizations with 38 in Fig. 2c (10 in Fig. 2d) models differing in their physics part

What is the mean:
-    mean of 164 (40) realizations or <--- this is meant by mean
-    mean of 48 (10) models?

a.

Regression Coefficient (unitless)

2 · 1.5 · 1 · 0.5 · 0 · -0.5 · -1 · -1.5 · -2 · -2.5

1900 · 1950 · 2000

Year

b.

2 · 1.5 · 1 · 0.5 · 0 · -0.5 · -1 · -1.5 · -2 · -2.5

1900 · 1950 · 2000

Year

QRA fingerprint (all-forcing)

c.

Regression Coefficient (unitless)

0.3 · 0.2 · 0.1 · 0 · -0.1 · -0.2 · -0.3

- QRA fingerprint
- rescaled 25-75N mean

1900 · 1950 · 2000

QRA fingerprint (anthro-only)

d.

0.5 · 0.4 · 0.3 · 0.2 · 0.1 · 0 · -0.1 · -0.2 · -0.3 · -0.4 · -0.5

1900 · 1950 · 2000

Figures 3
Projecting the quasi-resonant amplification (QRA) fingerprint (i.e. Fig. 1c) onto the CMIP5 zonal mean temperature profiles using linear regression (see Methods)
Figs. 3a & b: single model fingerprint. Each of the 48 (10) CMIP5 models is represented by a colored line.
                  multimodel average in Figs. 3a & b: black line. This black line is reproduced in Figs. 3c & d in a coordinate system zoom.
Figs. 3c & d: multimodel mean fingerprint

[*my comment*
Each single color zig-zac line in Figs. 3a&b is a ListPlot with PlotJoined->True of the
table_blue = Table[{{1860, regression coefficient_blue(1860)}, {1861, regression coefficient_blue(1861)}, {1862, regression coefficient_blue(1862)}, …{2015, regression coefficient_blue (2015)}}]
Similarly
table_yellow = Table[{{1860, regression coefficient_yellow(1860)}, …}]
Each Table could have been represented as series of dots, using ListPlot with PlotJoined->False.
]

… large amount of variability among the individual realizations of the multimodel ensemble … emphasizes the significant role of internal variability. ...

[*meaning*
If there was no such internal variability all the single realization zig-zacs would be locked into a synchronous pattern instead of moving independently from one another. Taking the mean of all realizations aims at
-    *averaging out this internal variability, thus*
-    *making visible the trend over the period 1860 - 2015.*
The rational behind taking the mean of all realizations (table-blue, table_yellow, …) instead of just one realization (e.g. table_blue) is the assumption that the mean shows a more reliable trend than any individual realization. This could well be wrong. It could well be that a group of realizations represents reality better than the rest of the realizations. In the extreme, none of the realizations might represent reality.]

… A positive long-term trend is nonetheless evident in most realizations, and is clearly evident in the ensemble means (Fig. 3a,b). This trend is formally independent of global warming, since it reflects a change over time in a relative latitudinal pattern of temperature variation rather than any change in mean hemispheric or global warmth. Comparing the ensemble mean fingerprint series to the ensemble mean extratropical (25–75N) mean temperature for the all-forcing simulations (Fig. 3c) nonetheless reveals a similar long-term increase consistent with polar amplification from anthropogenic warming.

Quasiresonant amplification of planetary waves and recent Northern Hemisphere weather extremes
Vladimir Petoukhov, Stefan Rahmstorf, Stefan Petri, and Hans Joachim Schellnhuber, Jan. 16, 2013
(PIK, Santa Fe Institute)
www.pnas.org/cgi/doi/10.1073/pnas.1222000110

Abstract
... we propose a common mechanism for the generation of persistent longitudinal planetary-scale high-amplitude patterns of the atmospheric circulation in the Northern Hemisphere midlatitudes.

Those patterns—with zonal wave numbers m = 6, 7, or 8—are characteristic of the above extremes [hot summers]. We show that these patterns might result from trapping within midlatitude waveguides of free synoptic waves with zonal wave numbers k ≈ m. Usually, the quasistationary dynamical response with the above wave numbers m to climatological mean thermal and orographic forcing is weak. Such midlatitude waveguides, however, may favor a strong magnification of that response through quasiresonance. … The data and results we present suggest that atmospheric conditions already might have changed to the extent that the considered quasiresonant wave amplification may occur rather frequently.

My introduction:
Using an equation approximating the air movement under the influence of
- *a pressure gradient force and*
- *the Coriolis force*

the generation of a waveguide and air flow within the waveguide is modeled. This system can develop discrete stationary jet stream patterns around the earth (much like resonances in a spatially confined system, e.g. the 2-D surface of a drum or the 3-D space of a cavity). Such jet stream patterns are actually found in CMIP5 model results (as published in daily NCEP–NCAR reanalysis data, see Kalnay E, et al. (1996) The NCEP-NCAR 40-year reanalysis project. Bull Am Meteorol Soc 77:437–470.)

I. Quasiresonance Hypothesis
Generally the large-scale midlatitude atmospheric circulation is characterized by
- (i) traveling *free synoptic-scale (few hundred to several thousand km) Rossby waves* with zonal wave numbers k ≥ 6 propagating predominantly in the longitudinal direction with the phase speed c ≈ 6 – 12m/s, and
- (ii) *quasistationary planetary-scale Rossby waves* with c ≈ 0, frequency ω ≈ 0, and various zonal wave numbers m as a response of atmospheric circulation to quasistationary (e.g., climatological mean) spatially inhomogeneous diabatic sources/sinks and orography.

The quasistationary component of midlatitude free synoptic-scale waves with k ≈ 6 – 8 normally is weak, with the magnitude of the meridional (north-south) velocity less than (1.5–2) m/s (26, 27). Below, k and m will denote the zonal wave numbers, respectively, of free synoptic waves and quasistationary planetary-scale Rossby waves mentioned above.

Our hypothesis is that during the extreme summer events considered, certain persistent high-amplitude wave structures evolved in the field of the large-scale midlatitude atmospheric meridional velocity (hereafter, V) to which the quasistationary component of free synoptic waves with k ≈ 6 – 8 made an exceptionally large contribution.

These structures may arise from changes in the midlatitude zonal (east-west) mean state. Namely, when the indicated changes lead to latitudinal trapping within the midlatitude waveguides of quasistationary free synoptic waves with k≈6–8, the usually weak midlatitude response of wave numbers m = 6; 7, and 8 to quasistationary thermal and orographic sources/sinks may be strongly magnified through quasiresonance.

quasi-resonance conditions
… only a near-zero leakage and absorption at the lateral boundaries of the waveguide of the wave energy for such a free wave can take place, provided that
(i) u>0, l2 >0 within the waveguide, and u>0, l2 <0 outside but in the vicinity of the waveguide.
As far as Eq. 2 is derived in the WKB approximation (20), two more requirements are imposed (29–31):
(ii) jdl–1=adφj<1 within the waveguide's internal part (interior), ΛW, implying that the change in the meridional wavelength Λφ for the trapped free wave over a distance Λφ=4π is small there compared with Λφ, and
(iii) the total width ΛW;t of the waveguide exceeds the characteristic scale ΔA of the relevant Airy function (29–31) for the considered trapped free wave
(iv) the meridional wave number l of this free synoptic wave falls into the range, Δlm, of the meridional wave numbers lm which gives a dominant contribution within ΛW to the combined amplitude A of the quasistationary orographic and m thermal terms in the right side of Eq. 1. … corresponding amplitude A of V may reach a high quasiresonant value for wave m number m in the case of k→m

from Wikipedia
The barotropic vorticity equation assumes the atmosphere is nearly barotropic, which means that the direction and speed of the geostrophic wind are independent of height. In other words, there is no vertical wind shear of the geostrophic wind. It also implies that thickness contours (a proxy for temperature) are parallel to upper level height contours. In this type of atmosphere, high and low pressure areas are centers of warm and cold temperature anomalies. Warm-core highs (such as the subtropical ridge and the Bermuda-Azores high) and cold-core lows have strengthening winds with height, with the reverse true for cold-core highs (shallow Arctic highs) and warm-core lows (such as tropical cyclones).[1]

The geostrophic wind is the theoretical wind that would result from an exact balance between the Coriolis force and the pressure gradient force. This condition is called geostrophic balance. The geostrophic wind is directed parallel to isobars (lines of constant pressure at a given height). This balance seldom holds exactly in nature. The true wind almost always differs from the geostrophic wind due to other forces such as friction from the ground. Thus, the actual wind would equal the geostrophic wind only if there were no friction and the isobars were perfectly straight. Despite this, much of the atmosphere outside the tropics is close to geostrophic flow much of the time and it is a valuable first approximation. Geostrophic flow in air or water is a zero-frequency inertial wave. … A useful heuristic is to imagine air starting from rest, experiencing a force directed from areas of high pressure toward areas of low pressure, called the pressure gradient force. If the air began to move in response to that force, however, the Coriolis "force" would deflect it, to the right of the motion in the northern hemisphere or to the left in the southern hemisphere. As the air accelerated, the deflection would increase until the Coriolis force's strength and direction balanced the pressure gradient force, a state called geostrophic balance. At this point, the flow is no longer moving from high to low pressure, but instead moves along isobars. Geostrophic balance helps to explain why, in the northern hemisphere, low-pressure systems (or cyclones) spin counterclockwise and high-pressure systems (or anticyclones) spin clockwise, and the opposite in the southern hemisphere.

Armin Fuchs

Nonlinear Dynamics in Complex Systems

Theory and Applications for the Life-, Neuro- and Natural Sciences

Springer, 2013 (cache)

Winter and Summer Rossby Wave Sources in the CMIP5 Models

Yu Nie1, Yang Zhang2, Xiu-Qun Yang2, and Hong-Li Ren1
1 Laboratory for Climate Studies, CMA-NJU Joint Laboratory for Climate Prediction Studies, National Climate Center, China Meteorological Administration, Beijing, China,
2 CMA-NJU Joint Laboratory for Climate Prediction Studies, Institute for Climate and Global Change Research, School of Atmospheric Sciences, Nanjing University, Nanjing, China

----

IPCC AR5

Working Group I Contribution to the Fifth Assessment Report of the Intergovernmental Panel on Climate Change
WG1AR5_all_final.pdf

page 2
In the WGI contribution to the AR5, uncertainty is quantified using 90% uncertainty intervals unless otherwise stated. The 90% uncertainty interval, reported in square brackets, is expected to have a 90% likelihood of covering the value that is being estimated. Uncertainty intervals are not necessarily symmetric about the corresponding best estimate. A best estimate of that value is also given where available.

page 88
TS.5.4.7   Possibility of Near-term Abrupt Changes in Climate
There are various mechanisms that could lead to changes in global or regional climate that are abrupt by comparison with rates experienced in recent decades. The likelihood of such changes is generally lower for the near term than for the long term. For this reason the relevant mechanisms are primarily assessed in the TS.5 sections on long-term changes and in TFE.5. {11.3.4}

page 140
climate is defined as an average over 30 years

WGIII AR5

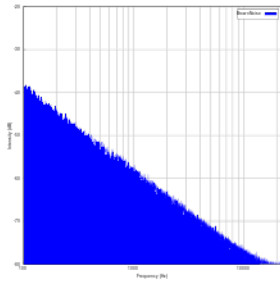
IPCC Glossary

https://www.ipcc.ch/site/assets/uploads/sites/3/2019/09/SROCC_FinalDraft_Annex1_Glossary.pdf

Climate variability   Deviations of some climate variables from a given mean state (including the occurrence of extremes, etc.) at all spatial and temporal scales beyond that of individual weather events. Variability may be intrinsic, due
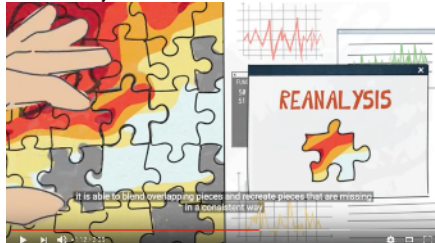- to fluctuations of processes internal to the climate system (**internal variability**), or
- to variations in natural or anthropogenic external forcing (forced variability).

Red noise (YouTube)

The graphic representation of the sound signal (or this signal) mimics a Brownian pattern. Its spectral density is inversely proportional to f^2, meaning it has more energy at lower frequencies, even more so than pink noise. It decreases in power by 6 dB per octave (20 dB per decade) and, when heard, has a "damped" or "soft" quality compared to white and pink noise. The sound is a low roar resembling a waterfall or heavy rainfall.

What is reanalysis?

(YouTube)

- Within the Copernicus Climate Change Service (C3S), ECMWF is producing a detailed record of the evolution of the global atmosphere from 1950 onwards, using a method called reanalysis. This meteorological dataset, ERA5, provides estimates of atmospheric parameters such as air temperature, pressure, wind, humidity and ozone at different altitudes, surface parameters such as rainfall, soil moisture, sea-surface temperature, … Reanalysis works in the same way, but at reduced resolution to allow for the provision of a dataset spanning back several decades. Reanalysis does not have the constraint of issuing timely forecasts, so there is more time to collect observations, and when going further back in time, to allow for the ingestion of improved versions of the original observations, which all benefit the quality of the reanalysis product. The assimilation system is able to estimate biases between observations and to sift good-quality data from poor data. The laws of physics allow for estimates at locations where data coverage is low, such as for surface temperature in the Arctic. The provision of estimates at each grid point around the globe for each regular output time, over a long period, always using the same format, makes reanalysis a very convenient and popular dataset to work with.(Source)